The Impact of Retardance Pattern Variability on Nerve Fiber Layer Measurements over Time Using GDx with Variable and Enhanced Corneal Compensation

Dilraj S. Grewal,[1] *Mitra Sehi,*[1] *Richard J. Cook,*[2] *David S. Greenfield,*[1] *and Advanced Imaging in Glaucoma Study Group*[3]

Purpose. To examine the impact of retardance pattern variability on retinal nerve fiber layer (RNFL) measurements over time using scanning laser polarimetry with variable (GDxVCC) and enhanced corneal compensation (GDxECC; both by Carl Zeiss Meditec, Inc., Dublin, CA).

Methods. Glaucoma suspect and glaucomatous eyes with 4 years of follow-up participating in the Advanced Imaging in Glaucoma Study were prospectively enrolled. All eyes underwent standard automated perimetry (SAP), GDxVCC, and GDxECC imaging every 6 months. SAP progression was determined with point-wise linear regression analysis of SAP sensitivity values. Typical scan score (TSS) values were extracted as a measure of retardance image quality; an atypical retardation pattern (ARP) was defined as TSS $<$ 80. TSS fluctuation over time was measured using three parameters: change in TSS from baseline, absolute difference (maximum minus minimum TSS value), and TSS variance. Linear mixed-effects models that accommodated the association between the two eyes were constructed to evaluate the relationship between change in TSS and RNFL thickness over time.

Results. Eighty-six eyes (51 suspected glaucoma, 35 glaucomatous) of 45 patients were enrolled. Twenty (23.3%) eyes demonstrated SAP progression. There was significantly greater fluctuation in TSS over time with GDxVCC compared with GDxECC as measured by absolute difference (18.40 $\pm$ 15.35 units vs. 2.50 $\pm$ 4.69 units; $P < 0.001$), TSS variance (59.63 $\pm$ 87.27 units vs. 3.82 $\pm$ 9.63 units, $P < 0.001$), and change in TSS from baseline (-0.83 ± 11.2 vs. 0.25 ± 2.9, $P = 0.01$). The change in TSS over time significantly ($P = 0.006$) influenced the TSNIT average RNFL thickness when measured by GDxVCC but not by GDxECC.

Conclusions. Longitudinal images obtained with GDxECC have significantly less variability in TSS and retardance patterns and have reduced bias produced by ARP on RNFL progression assessment. (*Invest Ophthalmol Vis Sci.* 2011;52:4516–4524) DOI:10.1167/iovs.10-5969

Scanning laser polarimetry (SLP) utilizes a confocal scanning laser ophthalmoscope with an integrated polarimeter and measures the amount of retardation (phase shift) of a polarized infrared laser beam as it passes through the retinal nerve fiber layer (RNFL). Linearly polarized light traversing the RNFL is elliptically polarized and the amount of linear retardation of light at each corresponding retinal location is proportional to the RNFL thickness.[1–3] Originally introduced in 1993, the first commercial SLP instrument used a fixed corneal compensation (GDxFCC; Laser Diagnostic Technologies, now Carl Zeiss Meditec, Dublin, CA) strategy that was based on population median values of corneal polarization axis and magnitude, to subtract anterior segment birefringence from total ocular birefringence. Subsequent experiments demonstrated that normal subjects have considerable variability in corneal birefringence properties, and correction for such variability improves the diagnostic precision of this technology.[1,4]

Variable corneal compensation (GDxVCC; Carl Zeiss Meditec, Inc.) was introduced in 2002. This methodology determined and neutralized eye-specific corneal polarization axis and magnitude using the concept of the macula as an intraocular polarimeter.[5–7] Atypical retardance patterns (ARPs) have been observed by GDxVCC in a subset of normal and glaucomatous eyes and are characterized as alternating bands of increased and decreased retardation, particularly in the nasal and temporal parapapillary region.[8,9] ARPs are observed more commonly in eyes of elderly patients or in eyes with lightly pigmented fundi with myopia.[10] Such images deviate from the normal pattern of birefringence, generally characterized by increased peripapillary birefringence superiorly and inferiorly that correspond histologically to the distribution of the superior and inferior arcuate nerve fiber bundles. The artifact introduced by ARP produces spurious RNFL thickness measurements and reduces the power to discriminate between healthy and glaucomatous eyes.[9–12]

The TSS is a support vector machine value that has been reported to be highly predictive of ARP, with a TSS $<$80 demonstrating good specificity and sensitivity for detection of ARP.[8] Recently, Medeiros et al.[13] demonstrated that, with GDxVCC, retardance pattern variability over time had a significant influence on the detection of progressive RNFL thickness loss. They suggested that eyes with ARP or large fluctuations in TSS over time may show false glaucomatous progression or that glaucomatous changes in RNFL thickness may be masked.

From the [1]Bascom Palmer Eye Institute, Department of Ophthalmology, University of Miami Miller School of Medicine, Palm Beach Gardens, Florida; and the [2]Department of Statistics and Actuarial Science, University of Waterloo, Waterloo, Ontario, Canada.

[3]Members of the Advanced Imaging in Glaucoma Study Group are listed in the Appendix.

Presented at the annual meeting of the Association for Research in Vision and Ophthalmology, Fort Lauderdale, Florida, May 2010.

Supported in part by National Institutes of Health Grant R01-EY013516, Bethesda, Maryland; the Maltz Family Endowment for Glaucoma Research, Cleveland, Ohio; a grant from Barney Donnelley, Palm Beach, Florida; The Kessel Foundation, Bergenfield, New Jersey; and an unrestricted grant from Research to Prevent Blindness, New York, New York.

Submitted for publication May 28, 2010; revised October 9 and December 15, 2010; accepted December 17, 2010.

Disclosure: **D.S. Grewal**, None; **M. Sehi**, None; **R.J. Cook**, None; **D.S. Greenfield**, Carl Zeiss Meditec (F), Topcon (C), Optovue (C)

Corresponding author: David S. Greenfield, Bascom Palmer Eye Institute, University of Miami Miller School of Medicine, 7101 Fairway Drive, Palm Beach Gardens, FL 33418; dgreenfield@med.miami.edu.

An enhancement module (enhanced corneal compensation, ECC) has been described to improve the signal-to-noise ratio and eliminate artifacts associated with ARP.[14,15] The ECC algorithm introduces a predetermined birefringence bias to shift the measurement of the total retardation to a higher value region to remove noise and reduce atypical patterns.[14–16] The amount of birefringence bias is determined using the birefringence pattern of the macular region and then is mathematically removed point by point from the total birefringence pattern of the VCC, to improve the signal and obtain a retardation pattern of the RNFL with the least noise. GDxECC has been demonstrated to increase the diagnostic accuracy of SLP.[15,17–19]

We hypothesized that longitudinal images obtained with GDxECC would have significantly less ARP, less variability in TSS and retardance patterns, and reduced bias produced by ARP on RNFL progression assessment. The purpose of this investigation was to evaluate the impact of retardance pattern variability on RNFL thickness measurements over time with the GDxVCC and GDxECC.

Patients and Methods

This was a prospective longitudinal cohort study. Participants consisted of patients with glaucoma or with suspected glaucoma who were prospectively enrolled in the Advanced Imaging in Glaucoma Study (AIGS) conducted at Bascom Palmer Eye Institute and were examined every 6 months. Informed consent was obtained from all subjects on a consent form approved by the Institutional Review Board of the University of Miami Miller School of Medicine, which is in agreement with the provisions of Declaration of Helsinki. Eyes meeting inclusion criteria with 4 years of follow-up were included. Inclusion criteria common to both groups consisted of spherical equivalent refractive error between −7.00 and +3.00 diopters sphere (DS), best corrected visual acuity (BCVA) of 20/40 or better, age between 40 and 79 years, and no history of intraocular surgery except for uncomplicated cataract extraction. Patients with ocular disease other than glaucoma or cataract, parapapillary atrophy extending to 1.7 mm from the center of the optic disc, unreliable SAP, or poor quality GDx images were excluded.

Eyes with suspected glaucoma were those with ocular hypertension characterized by intraocular pressure (IOP) ≥24 mm Hg with normal optic discs and normal results in standard automated perimetry (SAP) or patients with glaucomatous optic neuropathy on funduscopic examination and review of stereoscopic optic disc photographs but normal SAP results. Glaucomatous optic neuropathy was defined as neuroretinal rim narrowing to the optic disc margin, notching, excavation, or RNFL defect. Glaucoma patients had glaucomatous optic nerve damage and corresponding abnormal SAP defined as abnormal glaucoma hemifield test results and pattern standard deviation (PSD) outside 95% normal limits. Patients with SAP abnormalities had at least one confirmatory visual field examination. All patients underwent a baseline examination consisting of a complete ophthalmic examination, including slit lamp biomicroscopy, gonioscopy, Goldmann applanation tonometry, ultrasound pachymetry, dilated stereoscopic examination, photography of the optic disc, SAP, and GDx imaging. Follow-up SAP and GDx imaging were performed on the same day at 6-month intervals. During the follow-up period, each patient was treated at the discretion of the attending physician.

GDx Imaging and Analysis

GDx imaging was performed with the commercially available GDxVCC (Carl Zeiss Meditec, Inc., software ver. 6.0.0) in a standardized fashion through undilated pupils with both VCC and ECC. The instrument uses a laser beam with a wavelength of 785 nm to scan the ocular fundus, within a field of 40° horizontally × 20° vertically and a density of 256 × 128 pixels. In the ECC mode, the compensator is adjusted so that it combines with corneal birefringence to produce a bias retardation of approximately 55 nm with the slow axis close to the vertical axis. The software then measures a higher total retardation than the RNFL retardation alone, resulting in an improved signal-to-noise ratio. The actual bias retardation and the axis in each image are measured from the macular region and mathematically removed from the final RNFL image to determine the actual RNFL retardation.[9,16,17,20]

Three consecutive scans each were obtained with the GDxVCC and GDxECC, on the same day by the same operator. Two sets of GDx images were acquired at each visit, and the image with the highest quality was selected to be included in the analysis. A primary scan was obtained once before the baseline measurement to compensate for the corneal birefringence. A fixed concentric measurement band centered on the optic disc with a 3.2-mm outer and a 2.4-mm inner diameter was used to generate the peripapillary retardation measurements. Poor-quality SLP images (unfocused, poorly centered, obtained during eye movement, or Q score < 8) were excluded. The GDx parameters investigated in this study included the superior average, inferior average, and temporal–superior–nasal–inferior–temporal (TSNIT) average circumpapillary RNFL thicknesses measured using the automatically defined 3.2-mm diameter calculation circle. This parameter is provided on the standard GDxVCC and GDxECC printout. Nine GDx images with GDxVCC and nine with GDxECC were available for every patient.

The quality of the retardance image was quantified with a support vector machine score called the typical scan score (TSS, ranging from 0 to 100). ARP was defined as an SLP image with TSS < 80. TSS is based on the slope, standard deviation, and average magnitude of the RNFL thickness measurements from the edge of the optic nerve head extending outward to 20°. TSS fluctuation over the follow-up interval was quantified according to three parameters: change of TSS compared to baseline, absolute change in TSS (maximum minus minimum value), and the variance of TSS (SD^2).

Assessment of Progression by SAP

SAP was performed with the Swedish Interactive Threshold Algorithm (Humphrey Field Analyzer 750 II-i, 24-2 SITA Standard; Carl Zeiss Meditec, Dublin, CA). Only reliable test results (≤33% fixation losses, false-negative results, and false-positive results) were included. All patients were experienced with automated perimetry and had undergone a minimum of two visual field tests before study enrollment.

SAP progression was defined with progression detection software, with an automated pointwise linear regression analysis of SAP sensitivity values (Progressor software, ver. 3.3; Medisoft Inc., London, UK) that generates slopes to analyze the rate of global and local sensitivity change and the associated level of statistical significance.[20] Pointwise linear regression analysis of serial visual fields allows the longitudinal evaluation of sensitivity values at each test location over time. Progression was defined as the presence of at least one test point with a slope of sensitivity loss of >1 dB loss per year at $P < 0.01$, confirmed by at least one consecutive follow-up visual field test. For edge points, a stricter slope criterion of >2 dB loss per year (also at $P < 0.01$) was used.[21,22] The software provides an automated location of points with significant slopes of progression. Nine visual field results were included in the progression analyses for each patient.

Statistical Analysis

Statistical analysis was performed with commercial software (JMP, ver. 8.0 and SAS 9.0, SAS Inc., Cary, NC, and SPSS 17; SPSS, Chicago, IL). All tests were two-sided, and a result at $P < 0.05$ was significant. The independent-samples *t*-test, paired *t*-test, and χ^2 test were performed to compare clinical characteristics between groups. Linear mixed-effect models were constructed. These models were based on the longitudinal measurement of TSNIT average RNFL as the response. We used both fixed and random effects to investigate the longitudinal change in RNFL thickness over time as a function of TSS and its variability during the follow-up period. Categorical and continuous variables were simultaneously tested for their association with outcome measures as fixed effects. Covariates included in the model as fixed-effect parameters

TABLE 1. Baseline Clinical Characteristics of the Study Population

Parameter	Progressing Eyes (n = 20)	Nonprogressing Eyes (n = 66)	P
Age, y	65 ± 11.3	64.5 ± 9.3	
Sex			0.47†
Male	10	39	
Female	10	27	
Race			0.88*
White	14	52	
Hispanic	1	1	
Black	2	4	
Asian	3	9	
Central corneal thickness, μm	543.2 ± 44	556 ± 36.4	0.19*
Baseline IOP, mm Hg	17 ± 4.9	16.1 ± 3.4	0.48*
Baseline SAP, dB			
MD	−0.73 ± 1.6	−1.70 ± 3.36	0.08*
PSD	2.98 ± 2.88	2.62 ± 2.53	0.59*
GDxVCC			
TSNIT average RNFL, μm	51.26 ± 5.16	51.19 ± 5.53	0.96*
Baseline TSS, units	90.45 ± 15.19	83.83 ± 23.28	0.24*
GDxECC			
TSNIT average RNFL, μm	46.67 ± 4.63	49.02 ± 6.26	0.13*
Baseline TSS, units	100	98.86 ± 3.53	0.01*

n = 86 eyes.
* Independent-samples t-test.
† χ^2 test.

were time as a categorical variable; and TSS absolute difference, baseline TSS, variance of TSS, and change in TSS from baseline as continuous variables, with the latter being time-varying. The interaction between change in TSS and time was also included as a fixed effect. Random effects for "patient" and "eye nested within patient" were included in these models to accommodate serial dependence within eyes over time as well as associations between the left and right eyes. Separate models were constructed for GDxVCC and GDxECC responses. Each model was fit (1) for all eyes, (2) for progressing eyes, and (3) for nonprogressing eyes, as judged by the software (Progressor; Medisoft).

The following is the general equation used for these models:

$$Y_{i,j,k} = \beta_0 + \beta_1 \times \text{TSSabsolutedifference}_{i,j} + \beta_2 \times \Delta\text{TSS}_{i,j,k} + \beta_3 \times \Delta\text{TSS}_{i,j,k} \times \text{Time}_{i,j,k} + \beta_4 \times \text{TSSvariance}_{i,j} + \beta_5 \times \text{TSS}_{i,j} + \beta_6 \times \text{time}_{i,j,k} + b_j + b_{i,j} + \varepsilon_{i,j,k}$$

where $Y_{i,j,k}$ represents the individual measurement of TSNIT average RNFL for eye (j) of subject (i) at time point (k); β_0 to β_6 represent fixed effects associated with intercepts and the covariates included in the model; b_i corresponds to the random effect of patient; $b_{i,j}$ corresponds to random effect of eye (j) nested within patient; and $\varepsilon_{i,j}$ is the error component.

RESULTS

Eighty-six eyes (51 suspected glaucoma, 35 glaucoma) of 45 patients were enrolled (mean age, 64.7 ± 9.8, range 43–79 years). All eyes had a follow-up period of 4 years. Table 1 describes the clinical characteristics of the study population. Twenty (23.3%) eyes were characterized as progressing by the software (Progressor; Medisoft). The annual rate of RNFL loss (micrometers/year) for the TSNIT average, superior average, and inferior average parameters were significantly greater (P < 0.05) in progressing eyes than in nonprogressing eyes (Table 2). The rate of RNFL change with GDxVCC in nonprogressing eyes was positive and was associated with change in TSS over time. There was a significant correlation between the slope of TSNIT average (r = 0.49, P < 0.001), superior RNFL (r = 0.46, P < 0.001), and inferior RNFL (r = 0.33, P = 0.007), and the change in TSS at 48 months compared with baseline (baseline TSS minus TSS at 48 months) measured with GDxVCC in nonprogressing eyes.

We examined the relationship between change in structure and visual function over time. There was a significant correlation between the slope of superior RNFL detected by GDxVCC (r = −0.23, P < 0.001) and by GDxECC (r = −0.22, P < 0.001) and the number of progressing test locations in the inferior hemifield, and there was a significant correlation between the slope of inferior RNFL obtained with both GDxVCC (r = −0.10, P = 0.005) and GDxECC (r = −0.20, P < 0.001) and the number of progressing test locations in superior hemifield according to the progression detection software.

We examined the long-term fluctuation in TSS over time by GDxVCC and GDxECC. As shown in Table 3, the baseline TSS, absolute difference in TSS compared with baseline, and TSS variance were significantly ($P \leq 0.01$) greater with GDxVCC than with GDxECC. Figure 1 illustrates the absolute difference in TSS distributed among the study sample. GDxECC showed that 70 (81.4%) of 86 eyes had a ≤5-unit change in TSS over time, compared with GDxVCC, which showed 30 (34.9%) of 86 eyes demonstrating a >20-unit change in TSS.

TABLE 2. Difference in Rates of RNFL Thickness Loss (μm/y)

Rate of Change of RNFLT (μm/y)	Progressing Eyes (n = 20)	Nonprogressing Eyes (n = 66)	P*
GDxVCC			
TSNIT average	−0.47 ± 1.17	0.29 ± 0.95	0.004
Superior average	−0.79 ± 1.83	0.26 ± 1.16	0.003
Inferior average	−0.42 ± 1.70	0.45 ± 1.59	0.037
GDxECC			
TSNIT average	−0.75 ± 1.05	−0.18 ± 0.70	0.006
Superior average	−1.53 ± 1.46	−0.34 ± 1.09	<0.001
Inferior average	−1.07 ± 1.30	−0.22 ± 1.04	0.003

Progression was judged by Progressor (Medisoft, London, UK).
* Independent-samples t-test.

TABLE 3. Comparison of Baseline TSS and Variability in TSS Values

Parameter	GDxVCC	GDxECC	*P**
Baseline TSS, units*	85.37 ± 21.77 (13 to 100)	99.13 ± 3.12 (85 to 100)	<0.001
Change in TSS compared to baseline, (units)*	−0.83 ± 11.2 (−55 to 47)	0.25 ± 2.9 (−17 to 15)	0.01
Absolute difference in TSS (units)†	18.40 ± 15.35 (0 to 70)	2.50 ± 4.69 (0 to 18)	<0.001
TSS variance (SD^2)	59.63 ± 87.27 (0 to 471)	3.82 ± 9.63 (0 to 49)	<0.001

Baseline data are expressed as the mean ± SD, with the range in parentheses.
* Paired samples *t*-test.
† Maximum minus minimum TSS during follow-up.

With GDxVCC, 65 (75.6%) of 86 eyes had a normal retardance pattern at baseline, whereas 21 (24.4%) of 86 eyes had ARP. Eyes with baseline ARP (17 of 21 eyes, 81%) had a significantly greater ($P < 0.001$, Fisher's exact test) frequency of absolute TSS change >20 units during 4 years compared with eyes with a normal retardance pattern at baseline (13/65 eyes, 20%). GDxECC showed no ARP in any of the eyes at baseline or at any point during the follow-up period.

Table 4 shows results of the linear mixed-effects models investigating the influence of TSS on TSNIT average RNFL thickness over time. The eyes were subdivided based on the presence or absence of visual field progression. GDxVCC results showed that time had a significant ($P \leq 0.01$) impact on longitudinal measurements of TSNIT average RNFL in both progressing and nonprogressing eyes, and GDxECC showed an effect in all eyes and progressing eyes. GDxVCC showed a significant impact of the interaction between change in TSS from baseline and time on longitudinal measurements of average RNFL in all eyes ($P = 0.006$) and nonprogressing eyes ($P = 0.025$), and GDxECC showed the same association in progressing eyes ($P = 0.025$). Figure 2 demonstrates the relationship between the change in TSS from baseline and the change in TSNIT average RNFL from baseline in GDxVCC (Fig. 2A) and GDxECC (Fig. 2B) measurements. With GDxVCC, a significant inverse relationship was observed between the change in TSS and the change in TSNIT average RNFL thickness from baseline ($P < 0.001$), but not with GDxECC ($P = 0.07$). The rate of RNFL decline shown by GDxVCC (0.13 μm/year) was 13-fold greater for every 1-unit increase in TSS score per year than that shown by GDxECC (0.01 μm/year).

Figure 3 illustrates a case of a glaucomatous eye falsely identified by GDX VCC as having apparent RNFL loss over time, despite nonprogressing visual fields and optic disc stereophotographs. The baseline GDxVCC image (TSS 14) demonstrated ARP, and during 4 years of follow-up, there was a 32-unit increase in TSS and a 5.19 μm reduction in the TSNIT average RNFL thickness. The baseline GDxECC image demonstrated a normal retardance pattern (TSS = 91), and the absolute change in TSS was 7 units with less fluctuation in RNFL thickness.

Figure 4 illustrates a glaucomatous eye with superior visual field progression according to the detection software (Progressor; Medisoft) and a corresponding inferiorly located optic disc hemorrhage (white arrow) at 4 years of follow-up. The baseline GDxVCC image showed a normal retardance pattern (TSS = 91), and over 4 years of follow-up, there was a 24-unit reduction in TSS and an apparent 3.43 μm increase in the TSNIT average RNFL thickness. GDxECC showed no change in the absolute TSS over time and a 9.9-μm reduction in TSNIT average was observed for atrophy in the inferior region (black arrow) corresponding to the location of the optic disc hemorrhage and visual field change.

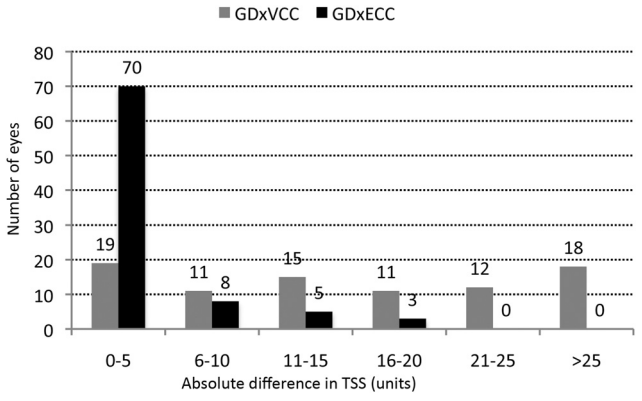

FIGURE 1. Absolute difference in TSSs obtained with GDxVCC and GDxECC, distributed among the study population.

DISCUSSION

Computerized imaging of the optic nerve and RNFL thickness has emerged as a useful tool to assist the clinician with documentation of glaucomatous structural damage and glaucoma risk assessment and to facilitate early diagnosis.[23] First described in 2005,[8] eyes with ARP have plagued the clinician seeking to use the GDxVCC to facilitate glaucoma diagnosis. The clinical consequence of ARP is that the artifact results in a falsely greater measured RNFL thickness and may mask glaucomatous RNFL thickness loss.[12,15] Such eyes are often myopic, with regions of retinal pigment epithelium atrophy, and generate considerable scleral reflectance and scatter that is thought to contribute to the underlying mechanism.[10]

In a recent study, Medeiros et al.[13] highlight additional concern regarding the impact of GDxVCC images containing ARP. They studied 377 eyes (suspected glaucoma and glaucomatous) longitudinally, with a median follow-up of 4 years, and demonstrated that eyes with ARP had a significant effect on detection of progressive RNFL loss. ARP was common with almost 20% of all eyes characterized by TSS <80. Lower TSSs at baseline were significantly associated with greater changes in scores over time; each unit of TSS change was associated with a 0.14-μm difference in TSNIT average over time. Eyes with baseline TSS <80 had a 50% likelihood of undergoing a 10-unit change in TSS, compared with eyes with TSS ≥80, which had a 14% likelihood.

In the present study, we found that GDxVCC showed ARP in a large percentage of eyes, but the phenomenon was not observed in any of the eyes imaged with GDxECC during the 4 years of follow-up. We found that eyes with atypical patterns at baseline had substantial variation in retardance pattern over time, as measured by the TSS. In our study, GDxVCC showed that 81% of eyes with baseline ARP had an absolute TSS change >20 units during the follow-up period compared with only

TABLE 4. Results of the Linear Mixed-Effects Models

Parameter	TSNIT Average RNFL by GDxVCC						TSNIT Average RNFL by GDxECC					
	All Eyes ($n_{patient}$ = 44, n_{eye} = 86)		Nonprogressing Eyes ($n_{patient}$ = 40, n_{eye} = 66)		Progressing Eyes ($n_{patient}$ = 17, n_{eye} = 20)		All Eyes ($n_{patient}$ = 44, n_{eye} = 86)		Nonprogressing Eyes ($n_{patient}$ = 40, n_{eye} = 66)		Progressing Eyes ($n_{patient}$ = 17, n_{eye} = 20)	
	EST (SE)	*P*	EST (SE)	*P*	EST (SE)	*P*	EST (SE)	*P*	EST (SE)	*P*	EST (SE)	*P*
Intercept	50.369 (0.726)	<0.001	49.876 (0.768)	<0.001	52.166 (1.777)	<0.001	47.320 (0.833)	<0.001	47.564 (0.915)	<0.001	46.550 (1.222)	<0.001
Time	0.153 (0.105)	0.145	0.381 (0.115)	0.001	−0.603 (0.237)	0.012	−0.168 (0.079)	0.035	−0.003 (0.090)	0.974	−0.863 (0.175)	<0.001
Absolute Difference in TSS	0.123 (0.124)	0.325	0.053 (0.155)	0.732	0.011 (0.228)	0.965	0.575 (0.251)	0.025	0.680 (0.259)	0.012	0.799 (0.608)	0.208
Change in TSS	0.003 (0.033)	0.940	−0.021 (0.035)	0.553	0.117 (0.096)	0.225	−0.116 (0.096)	0.227	−0.167 (0.098)	0.090	1.536 (0.651)	0.020
Change in TSS × time	−0.029 (0.010)	0.006	−0.024 (0.011)	0.025	−0.056 (0.030)	0.064	−0.005 (0.032)	0.879	−0.007 (0.032)	0.827	−0.543 (0.239)	0.025
Baseline TSS	−0.057 (0.039)	0.148	−0.058 (0.041)	0.162	−0.093 (0.118)	0.444	−0.026 (0.230)	0.912	−0.003 (0.243)	0.989	*	*

Absolute difference of TSS: maximum minus minimum TSS during the follow-up period; EST, estimate of regression coefficient; SE, standard error for the regression coefficient.
* Since the baseline TSS values of GDxECC in progressing eyes (n = 17) were all 100, the estimate of regression coefficient could not be calculated.

FIGURE 2. Scatterplots demonstrate the relationship between the change in typical scan score (TSS) from baseline and the change in TSNIT average RNFL from baseline in GDxVCC (**A**) and GDxECC (**B**) scans in all eyes. A significant inverse relationship was observed between the change in TSS and the change in TSNIT average RNFL thickness from baseline in GDxVCC ($P < 0.001$) but not in GDxECC ($P = 0.07$) measurements.

20% of eyes with normal retardation patterns at baseline. Similarly, with GDxVCC, changes in retardation pattern over time correlated highly with RNFL thickness assessment, and there was an inverse relationship between TSS and measured RNFL thickness. Conversely, eyes imaged with GDxECC had little variability in TSS during the follow-up period, with 81% of eyes having ≤5-unit change in TSS. No relationship was observed between any measure of long-term TSS fluctuation and RNFL thickness assessment over time.

Previous cross-sectional studies have compared GDxECC and GDxVCC and have shown improved diagnostic accuracy and stronger structure function relationships in glaucomatous eyes with GDxECC.[18,19,24–27] Medeiros et al.[13] prospectively evaluated the impact of ARP on detection of progressive RNFL loss with GDxVCC. There are several differences between our study and the report by Medeiros et al. We examined the

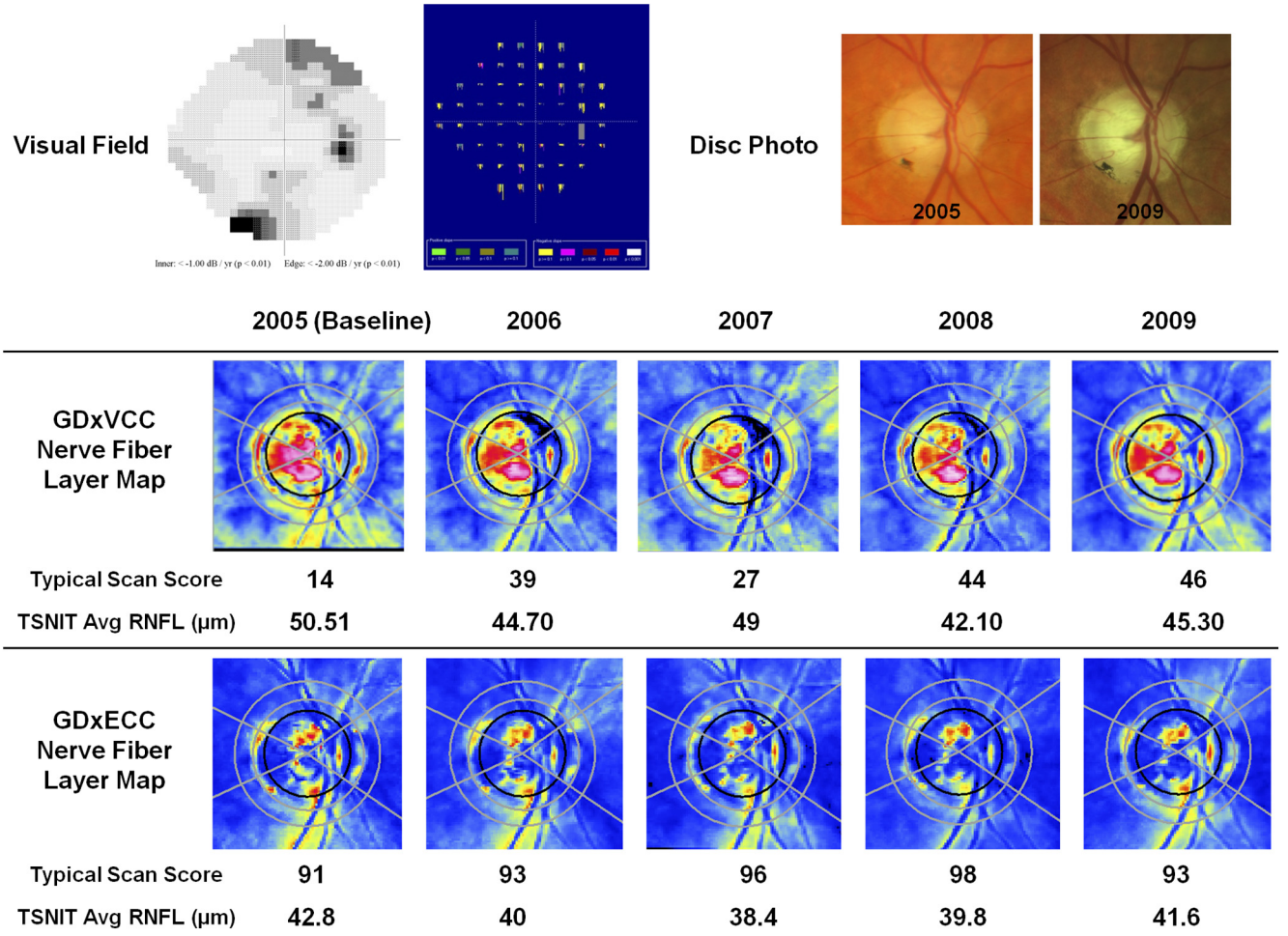

FIGURE 3. A glaucomatous eye falsely identified as having apparent RNFL loss over time by GDxVCC, despite nonprogressing visual fields (*top left*) and optic disc stereophotographs (*top right*). On the detection software map (Progressor Medisoft, London, UK), each bar represents one test with the bar length showing to the depth of the defect and the color showing the *P* value of the regression slope. None of the locations demonstrated progression in this patient. The baseline GDxVCC (*middle*) image (TSS = 14) demonstrated ARP, and during 4 years of follow-up, there was a 32-unit increase in TSS and a 5.19-μm reduction in the TSNIT average RNFL thickness. The baseline GDxECC image (*bottom*) demonstrated a normal retardance pattern (TSS 91), and the absolute change in TSS was 7 units with less fluctuation in RNFL thickness.

impact of retardation pattern stability on longitudinal RNFL thickness measurements obtained with GDxVCC and GDxECC, to compare TSS variability over time and quantify the impact of retardance pattern variability on progression judgment. We used different methods to analyze visual field progression. Medeiros et al. defined visual field progression with an event-based analysis using guided progression analysis software (Carl Zeiss Meditec, Dublin, CA), which identifies sensitivity loss on three consecutive examinations compared with baseline. We defined visual field progression with a trend-based method using pointwise linear regression analysis of all available visual fields to identify significant localized sensitivity loss. In a more recent study Medeiros et al.[28] used both GDxVCC and GDxECC to examine the impact of ARP on progressive RNFL loss but did not measure TSS variance over time. Despite the methodological differences among these studies, similar conclusions may be derived regarding the high variability of TSS with GDxVCC and the impact of ARP on judgment of RNFL change over time.

We compared the impact of retardation pattern stability on longitudinal RNFL thickness measurements by two corneal compensation methodologies. Longitudinal changes in TSS were inversely related to changes in RNFL thickness using GDxVCC, whereas such changes did not influence RNFL thickness measurements using GDxECC. We found that each 1-unit increase in TSS per year was associated with a 0.13-μm decline in RNFL thickness per year with GDxVCC, which was 13 times greater than the 0.01-μm decline observed with GDxECC. Thus, a 20-unit change in TSS over 4 years, which occurred in approximately one third of eyes using GDxVCC in our study, would result in a 2.6-μm change in RNFL over the 4-year period (0.65 μm/yr). The implication of this bias has considerable relevance with regard to clinical assessment of progression. Glaucoma represents an accelerated loss of retinal ganglion cells and axons, beyond the normal age-related decline observed among normal subjects estimated to be 5000 ganglion cells/year.[29] With GDxVCC measurements, age-related decline in RNFL has been reported to be approximately 0.1 μm/year.[30] In our study, GDxVCC showed a mean rate of average RNFL loss of 0.47 μm/year in eyes with SAP progression, and GDxECC showed a loss of 0.75 μm/year. This suggests that the absence of longitudinal influence of TSS over time on RNFL thickness measurements by GDxECC provides increased ability of this methodology to detect RNFL loss that exceeds age-related change and would be expected to increase the structure function relationship in progressing eyes.

The high frequency of eyes (30/86, 35%) that showed large variability in TSS raises both concern and questions about the

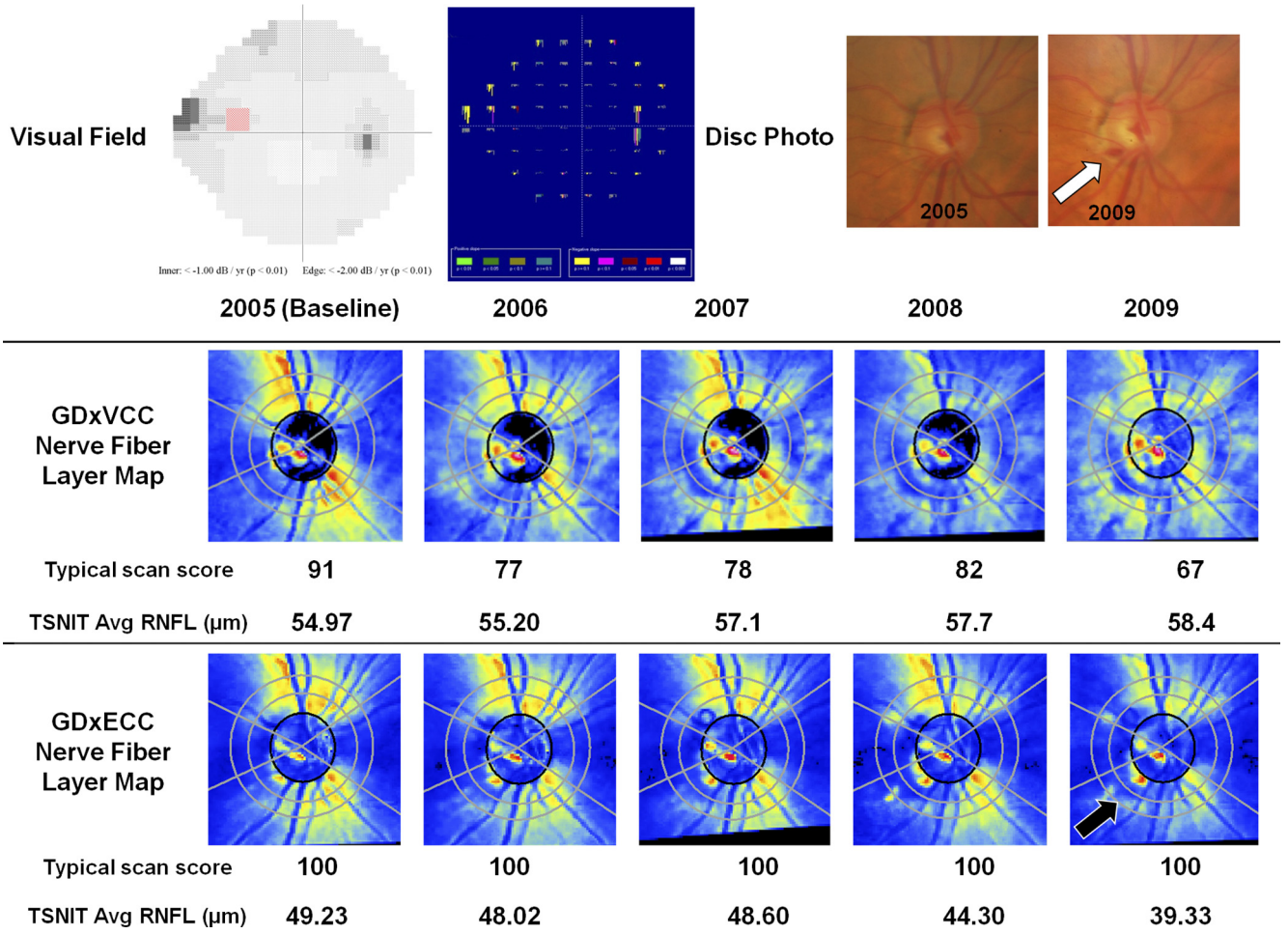

Figure 4. A glaucomatous eye with superior visual field progression (*top left*) as judged with progression detection software (Progressor; Medisoft, London, UK) and a corresponding inferiorly located optic disc hemorrhage (*top right*, *arrow*) at 4 years of follow-up. The progressing point is highlighted in *red* on the gray-scale image and is seen as a series of progressively lengthening bars on the software-generated map, which are color coded in *red* when the regression slope becomes significant ($P < 0.01$). The baseline GDxVCC (*middle*) image showed a normal retardance pattern (TSS = 91), and during 4 years of follow-up, there was a 24-unit reduction in TSS and an apparent 3.43-μm increase in the TSNIT average RNFL thickness. GDxECC (*bottom*) showed no change in the absolute TSS over time, and a 9.9-μm reduction in TSNIT average was observed with atrophy in the inferior region (*black arrow*) corresponding to the location of the optic disc hemorrhage and visual field change.

underlying mechanism of ARP. Why would the magnitude of scleral scatter within a given eye markedly change in a relatively short time frame of 4 years? To what degree does eye position or testing conditions contribute to the source of variability? Does instrument calibration play a role? Axial length, myopia, and the quality of the sclera have been suggested as sources of ARP[31,32]; however, the pathophysiology of ARP images is not entirely known. It has been hypothesized that such images occur in the presence of low signal-to-noise ratio resulting from loss or diminution of reflectivity from the retinal pigment epithelium. The low signal-to-noise ratio produces an increased gain to augment the polarization signal, which paradoxically increases noise from deeper retinal structures such as the sclera. Our results demonstrate that newer methods for corneal compensation such as ECC reduce the prevalence of TSS variability and therefore reduce the bias contributed to longitudinal RNFL thickness assessment.

The relationship between ARP and cataract is unclear. In theory, it is plausible that lens opacification degrades the signal-to-noise ratio and adversely affects TSS. Brittain et al.[33] demonstrated improvement in mean TSS after YAG laser capsulotomy (mean TSS of 33 before and 55 after laser) in eyes with posterior capsular opacification. However, their results demonstrate that the birefringence patterns remain atypical despite improvement in media clarity. As cataract grading was not performed in our study, prospective studies are warranted, to study the longitudinal impact of cataract grade and location on birefringence quality.

The results of this study have several important clinical consequences. Most important, clinicians should measure TSS in all eyes that undergo GDxVCC imaging. Although a Q-score is provided on the GDxVCC printout, representing a quality score (based on image focus, motion artifact, centration, and illumination), the quality of corneal compensation must be measured using the TSS and eyes with values below 80 should be avoided due to artifact that will bias not only the diagnosis of glaucoma but also the judgment of progression. Moreover, the assessment of glaucomatous progression in eyes with a large change in TSS should be avoided due to significant bias. As illustrated in Figures 3 and 4, GDxVCC may produce false identification of RNFL loss in nonprogressive glaucomatous eyes with baseline ARP and subsequent increased TSS (e.g., a shift in the direction of normal retardance pattern) during the follow-up interval. Conversely, detection of RNFL thickness loss may be masked in glaucomatous eyes with confirmed SAP progression by progressive reduction in TSS values (e.g., a shift

in the direction of ARP) when the baseline GDxVCC retardance pattern is normal. In both cases, RNFL thickness assessment with GDxECC was not influenced by longitudinal changes in TSS.

All technologies may falsely identify glaucomatous change, and identifying sources of artifact is critical. This study emphasizes the importance of image quality when interpreting GDxVCC images in clinical practice and adds to our understanding of RNFL thickness changes that may occur in eyes with progressive and nonprogressive glaucomatous optic neuropathy. In conclusion, clinicians must exert caution when using the GDxVCC for longitudinal evaluation of RNFL thickness in eyes with significant variability in TSS over time. GDxECC has a distinct advantage over GDxVCC, since longitudinal assessment of RNFL thickness change is not significantly influenced by changes in retardation patterns, which suggests that this methodology should provide more robust assessment of glaucomatous structural progression.

Acknowledgments

The authors are grateful to Ker-Ai Lee, M.Math (Department of Statistics and Actuarial Science, University of Waterloo, Canada), for assistance with the statistical modeling.

References

1. Greenfield DS, Knighton RW, Huang XR. Effect of corneal polarization axis on assessment of retinal nerve fiber layer thickness by scanning laser polarimetry. *Am J Ophthalmol.* 2000;129:715–722.
2. Knighton RW, Huang XR, Greenfield DS. Analytical model of scanning laser polarimetry for retinal nerve fiber layer assessment. *Invest Ophthalmol Vis Sci.* 2002;43:383–392.
3. Knighton RW, Huang X, Zhou Q. Microtubule contribution to the reflectance of the retinal nerve fiber layer. *Invest Ophthalmol Vis Sci.* 1998;39:189–193.
4. Weinreb RN, Bowd C, Greenfield DS, Zangwill LM. Measurement of the magnitude and axis of corneal polarization with scanning laser polarimetry. *Arch Ophthalmol.* 2002;120:901–906.
5. Weinreb RN, Bowd C, Zangwill LM. Glaucoma detection using scanning laser polarimetry with variable corneal polarization compensation. *Arch Ophthalmol.* 2003;121:218–224.
6. Bagga H, Greenfield DS, Knighton RW. Scanning laser polarimetry with variable corneal compensation: identification and correction for corneal birefringence in eyes with macular disease. *Invest Ophthalmol Vis Sci.* 2003;44:1969–1976.
7. Poinoosawmy D, Tan JC, Bunce C, Hitchings RA. The ability of the GDx nerve fibre analyser neural network to diagnose glaucoma. *Graefes Arch Clin Exp Ophthalmol.* 2001;239:122–127.
8. Bagga H, Greenfield DS, Feuer WJ. Quantitative assessment of atypical birefringence images using scanning laser polarimetry with variable corneal compensation. *Am J Ophthalmol.* 2005;139:437–446.
9. Da Pozzo S, Marchesan R, Canziani T, Vattovani O, Ravalico G. Atypical pattern of retardation on GDx-VCC and its effect on retinal nerve fibre layer evaluation in glaucomatous eyes. *Eye (Lond).* 2006;20:769–775.
10. Orlev A, Horani A, Rapson Y, Cohen MJ, Blumenthal EZ. Clinical characteristics of eyes demonstrating atypical patterns in scanning laser polarimetry. *Eye (Lond).* 2008;22:1378–1383.
11. Mai TA, Reus NJ, Lemij HG. Diagnostic accuracy of scanning laser polarimetry with enhanced versus variable corneal compensation. *Ophthalmology.* 2007;114:1988–1993.
12. Bowd C, Medeiros FA, Weinreb RN, Zangwill LM. The effect of atypical birefringence patterns on glaucoma detection using scanning laser polarimetry with variable corneal compensation. *Invest Ophthalmol Vis Sci.* 2007;48:223–227.
13. Medeiros FA, Alencar LM, Zangwill LM, Sample PA, Susanna Jr R, Weinreb RN. Impact of atypical retardation patterns on detection of glaucoma progression using the GDx with variable corneal compensation. *Am J Ophthalmol.* 2009;148:155–163.e151.
14. Toth M, Hollo G. Enhanced corneal compensation for scanning laser polarimetry on eyes with atypical polarisation pattern. *Br J Ophthalmol.* 2005;89:1139–1142.
15. Sehi M, Guaqueta DC, Greenfield DS. An enhancement module to improve the atypical birefringence pattern using scanning laser polarimetry with variable corneal compensation. *Br J Ophthalmol.* 2006;90:749–753.
16. Reus NJ, Zhou Q, Lemij HG. Enhanced imaging algorithm for scanning laser polarimetry with variable corneal compensation. *Invest Ophthalmol Vis Sci.* 2006;47:3870–3877.
17. Sehi M, Guaqueta DC, Feuer WJ, Greenfield DS. Scanning laser polarimetry with variable and enhanced corneal compensation in normal and glaucomatous eyes. *Am J Ophthalmol.* 2007;143:272–279.
18. Medeiros FA, Bowd C, Zangwill LM, Patel C, Weinreb RN. Detection of glaucoma using scanning laser polarimetry with enhanced corneal compensation. *Invest Ophthalmol Vis Sci.* 2007;48:3146–3153.
19. Mai TA, Reus NJ, Lemij HG. Structure-function relationship is stronger with enhanced corneal compensation than with variable corneal compensation in scanning laser polarimetry. *Invest Ophthalmol Vis Sci.* 2007;48:1651–1658.
20. Viswanathan AC, Fitzke FW, Hitchings RA. Early detection of visual field progression in glaucoma: a comparison of PROGRESSOR and STATPAC 2. *Br J Ophthalmol.* 1997;81:1037–1042.
21. Strouthidis NG, Scott A, Peter NM, Garway-Heath DF. Optic disc and visual field progression in ocular hypertensive subjects: detection rates, specificity, and agreement. *Invest Ophthalmol Vis Sci.* 2006;47:2904–2910.
22. Crabb DP, Fitzke FW, McNaught AI, Edgar DF, Hitchings RA. Improving the prediction of visual field progression in glaucoma using spatial processing. *Ophthalmology.* 1997;104:517–524.
23. Greenfield DS, Weinreb RN. Role of optic nerve imaging in glaucoma clinical practice and clinical trials. *Am J Ophthalmol.* 2008;145:598–603.
24. Bowd C, Tavares IM, Medeiros FA, Zangwill LM, Sample PA, Weinreb RN. Retinal nerve fiber layer thickness and visual sensitivity using scanning laser polarimetry with variable and enhanced corneal compensation. *Ophthalmology.* 2007;114:1259–1265.
25. Choi J, Kim KH, Lee CH, et al. Relationship between retinal nerve fibre layer measurements and retinal sensitivity by scanning laser polarimetry with variable and enhanced corneal compensation. *Br J Ophthalmol.* 2008;92:906–911.
26. Morishita S, Tanabe T, Yu S, et al. Retinal nerve fibre layer assessment in myopic glaucomatous eyes: comparison of GDx variable corneal compensation with GDx enhanced corneal compensation. *Br J Ophthalmol.* 2008;92:1377–1381.
27. Kim KH, Choi J, Lee CH, Cho BJ, Kook MS. Relationship between scanning laser polarimetry with enhanced corneal compensation and with variable corneal compensation. *Kor J Ophthalmol.* 2008;22:18–25.
28. Medeiros FA, Zangwill LM, Alencar LM, Sample PA, Weinreb RN. Rates of progressive retinal nerve fiber layer loss in glaucoma measured by scanning laser polarimetry. *Am J Ophthalmol.* 2010;149:908–915.
29. Balazsi AG, Rootman J, Drance SM. The effect of age on the nerve fiber population of the human optic nerve. *Am J Ophthalmol.* 1984;97:760–766.
30. Da Pozo S, Tacono P, Marchesan R, Minutola D, Ravalico G. The effect of ageing on retinal nerve fibre layer thickness: an evaluation by scanning laser polarimetry with variable corneal compensation. *Acta Ophthalmologica Scandinavica.* 2006;84:375–379.
31. Gotzinger E, Pircher M, Baumann B, Hirn C, Vass C, Hitzenberger CK. Analysis of the origin of atypical scanning laser polarimetry patterns by polarization-sensitive optical coherence tomography. *Invest Ophthalmol Vis Sci.* 2008;49:5366–5372.
32. Qiu K, Leung CKS, Weinreb RN, et al. Predictors of atypical birefringence pattern in scanning laser polarimetry. *Br J Ophthalmol.* 2009;93:1191–1194.
33. Brittain CJ, Fong KC, Hull CC, Gillespie IH. Changes in scanning laser polarimetry before and after laser capsulotomy for posterior capsular opacification. *J Glaucoma.* 2007;16:112–116.

APPENDIX

Advanced Imaging in Glaucoma Study Group

Bascom Palmer Eye Institute, *Department of Ophthalmology*, *University of Miami Miller School of Medicine*, *Palm Beach Gardens*, *Florida*: David S. Greenfield, Mitra Sehi, Krishna Kishor, and Carolyn D. Quinn.

University of Pittsburgh Medical Center, *Department of Ophthalmology*, *University of Pittsburgh School of Medicine*, *Pittsburgh*, *Pennsylvania*: Joel S. Schuman, Robert J. Noecker, Hiroshi Ishikawa, Gadi Wollstein, Richard A. Billonick, and Larry Kagemann.

Doheny Eye Institute, *Department of Ophthalmology*, *University of Southern California Keck School of Medicine*, *Los Angeles*, *California*: David Huang, Rohit Varma, Vikas Chopra, Brian Francis, Kenneth L. Lu, Ou Tan, and Srinivas R. Sadda.

See www.AIGStudy.net for the full list of the study group members.